Thermodynamic and electromagnetic properties of a spin-glass superconductor

E. J. Nicol and J. P. Carbotte
Department of Physics, McMaster University, Hamilton, Ontario, Canada L8S 4M1
(Received 28 October 1991)

For an intrinsic spin-glass superconductor, we have calculated several thermodynamic and electromagnetic properties as a function of temperature. In particular, we present calculations of the free-energy difference between the normal and superconducting states, the electronic specific-heat difference, the London and local penetration depths, the electromagnetic coherence length, and the thin-film critical current. The results are sensitive to the spin-glass parameters assumed and are distinct from those of Abrikosov-Gor'kov theory for noninteracting spins.

I. INTRODUCTION

It is well known that materials that contain a dilute concentration of noninteracting paramagnetic impurities, which interact with the conduction electrons through spin-flip scattering in the weak-scattering limit, can be successfully described by the model of Abrikosov and Gor'kov.[1] However, although some materials can be described by such a model, there is a large body of physics devoted to the understanding of localized moments that interact with each other and undergo ordering to states such as ferromagnetism or antiferromagnetism.

Anderson and Suhl[2] have shown that the coexistence of these ordered states with superconductivity depends on whether the ordered state produces a macroscopic field on the scale of the coherence distance. In the case of ferromagnetism such a net field exists and superconductivity is not able to coexist due to the splitting of the spin-up and spin-down conduction electron bands by the magnetic field. On the other hand, antiferromagnetism and superconductivity are well known to coexist;[3] superconductivity is then uninhibited by the magnetic ordering as the net magnetic field of the moments averages to zero.

Another possible magnetic state occurs in substitutionally disordered alloys, where the localized magnetic moments are randomly distributed and interact via the long-range Rudermann-Kittel-Kasuya-Yosida (RKKY) interaction mediated by the conduction electrons. This produces frustration in the magnetic ordering as not all magnetic moments can be simultaneously satisfied in their spin orientation with respect to the others. This leads to an infinite number of random configurations that are degenerate in energy but separated by large energy barriers so that one ground state cannot evolve into another on the laboratory time scale. These materials are known as spin glasses, of which Ag-Mn and Cu-Mn are examples of canonical metallic spin glasses. Coexistence of superconductivity and spin-glass ordering has been observed by Davidov *et al.*[4] in $Gd_xTh_{1-x}Ru_2$, $Gd_xCe_{1-x}Ru_2$, and $Gd_xLa_{3-x}In$.

Associated with the spin-glass state is a characteristic temperature T_f (the freezing temperature) below which the spins "freeze" into one of these random configurations. Spin glasses are characterized by a cusp in the magnetic susceptibility at T_f, no anomaly at T_f in the specific heat other than a broad maximum around T_f, and no Bragg peaks (which normally indicate long-range magnetic order) in neutron scattering experiments.

An attempt to describe the spin-glass phase was made by Edwards and Anderson.[5] As in all problems on phase transitions, one tries to identify an appropriate order parameter that will be nonzero in the phase of interest and zero in the disordered phase. Edwards and Anderson[5] introduced an order parameter which is related to the probability that a spin with a given direction at a time $t=0$ will have the same direction in the infinite-time limit. This order parameter reflects the "frozen" nature of the spin-glass state but has no spatial correlations as would be found in other magnetic order parameters.

Several reviews and books exist on the topic of spin glasses.[6-8] Here we will be following a particular model given by Nass *et al.*[9] and used more recently by Schachinger *et al.*,[10] Stephan and Carbotte,[11] and Perez Gonzalez *et al.*[12] We will be presenting results which extend the work of Stephan and Carbotte,[11] which was done in the context of BCS theory, to strong coupling theory. In addition, we examine several properties not previously investigated, in the work of Stephen and Carbotte.[11]

Before describing our calculations we will summarize the necessary theoretical background. First, we will briefly review the Eliashberg formulation of paramagnetic spin fluctuations and derive the limiting case of Abrikosov-Gor'kov paramagnetic impurities. Then we will introduce the model of Nass *et al.*[9] as it is imbedded in the Eliashberg notation.

II. THE THEORETICAL MODEL

Berk and Schrieffer[13] have given a model for incorporating paramagnetic spin-density fluctuations (paramagnons) into Eliashberg theory. It is based upon capturing the essence of how paramagnetic spin fluctuations are expected to affect spin-singlet pairing in a superconductor. Typically, due to strong Coulomb interactions between electrons in very narrow energy bands, ferromagnetic correlations (for example) may cause spin po-

larization of the electron cloud (a fluctuation in the spin density), such that an electron seeking to lower its energy by forming a Cooper pair in a spin-singlet state with another electron through the electron-phonon interaction (which is short range in real space), might actually be inhibited or repulsed by this cloud of polarized electrons of the wrong spin.[13] This forms a repulsive interaction. Allen and Mitrović[14] have given a loose definition of paramagnons as "interacting electron-hole pairs of spin 1." Paramagnons are typically heavily damped excitations that cause strong renormalization effects.[15,16]

In this model, a standard set of Eliashberg equations for both phonons and paramagnons can be written.[13,17–23] The kernel in these equations is written in terms of the spectral density, $\alpha^2F(\omega)$, for the coupling of the electrons to the phonons and the analogous one for paramagnons, $P(\omega)$. As paramagnons are pair breaking (or repulsive), they enter the equation for the gap parameter with a negative sign relative to the pair-enhancing phonons. However, in the renormalization equation, $P(\omega)$ enters with a plus sign and hence accentuates strong-coupling effects. The Eliashberg equations for the order parameter and renormalized frequencies of the superconducting state are given as[17,20–23]

$$\tilde{\Delta}_n=\pi T\sum_{m=-\infty}^{\infty}[\lambda^-(n-m)-\mu^*\theta(\omega_c-|\omega_m|)]\frac{\tilde{\Delta}_m}{\sqrt{\tilde{\omega}_m^2+\tilde{\Delta}_m^2}} \tag{1}$$

and

$$\tilde{\omega}_n=\omega_n+\pi T\sum_{m=-\infty}^{\infty}\lambda^+(n-m)\frac{\tilde{\omega}_m}{\sqrt{\tilde{\omega}_m^2+\tilde{\Delta}_m^2}}\ , \tag{2}$$

where

$$\lambda^{\pm}(n-m)\equiv\lambda^{\pm}(i\omega_m-i\omega_n)\equiv\int_0^{\infty}\frac{2\omega[\alpha^2F(\omega)\pm P(\omega)]}{\omega^2-(i\omega_m-i\omega_n)^2}d\omega\ , \tag{3}$$

and $\tilde{\Delta}_n\equiv\tilde{\Delta}(i\omega_n)=Z(i\omega_n)\Delta(i\omega_n)$ and $\tilde{\omega}_n=Z(i\omega_n)\omega_n$ with $i\omega_n\equiv i\pi T(2n+1)$, $n=0,\pm1,\pm2,\ldots,T$ is the temperature, and μ^* is the Coulomb pseudopotential. The spin fluctuation spectral density is related to the spin fluctuation propagator by[14,18]

$$P(\omega)=N(0)\sum_{k,k'}\left[-\frac{1}{\pi}\mathrm{Im}\chi^{+-}(k,k',\omega+i0^+)\right]\delta(\epsilon_k)\delta(\epsilon_{k'})\Big/\sum_{k,k'}\delta(\epsilon_k)\delta(\epsilon_{k'}) \tag{4}$$

$$=N(0)\int_0^{2k_F}\frac{q\,dq}{2k_F^2}\mathrm{Im}\mathcal{T}(q,\omega)\ , \tag{5}$$

where q is the momentum transferred, $N(0)$ is the single-spin density of states at the Fermi momentum, and in Eq. (5) a spherical Fermi surface has been assumed. The spin fluctuation propagator is related to the particle-hole $\mathcal{T}$ matrix through the Fourier transform of the transverse susceptibility $\chi^{+-}(q,\omega)$.[15,24] Our starting point will be at an assumed form for $P(\omega)$ and hence details of the microscopic theory beyond this point are unnecessary for our discussion.

The static limit of dynamic paramagnetic spin fluctuations are paramagnetic impurities that spin-flip scatter the electron. Like paramagnons, as paramagnetic impurities are pair breaking, they will cause a reduction in T_c over the pure case. These are described in the dilute, noninteracting limit by the theory of Abrikosov and Gor'kov,[1] where interaction between the moments on the magnetic atoms are neglected and single scattering events are assumed such that multiple scattering need not be considered. The strong scattering limit (which allows for the possibility of bound states being formed at the impurity sites) requires the theory of Shiba[25] and Rusinov,[26] who solved the problem exactly without the use of perturbation theory, but rather used the $\mathcal{T}$ matrix. Shiba-Rusinov theory reduces to Abrikosov-Gor'kov theory in the weak scattering limit. Here, we will only consider Abrikosov-Gor'kov theory, which has been examined by many authors.[27–30] In the end we will be interested in the case of interacting magnetic impurities described within the Abrikosov-Gor'kov formulation.

The Eliashberg equations for the Matsubara pairing energy $\tilde{\Delta}(i\omega_n)$ and renormalized frequencies $\tilde{\omega}(i\omega_n)$, incorporating such paramagnetic impurity scattering are given as[30]

$$\tilde{\Delta}_n=\pi T\sum_{m=-\infty}^{\infty}[\lambda(n-m)-\mu^*\theta(\omega_c-|\omega_m|)]\frac{\tilde{\Delta}_m}{\sqrt{\tilde{\omega}_m^2+\tilde{\Delta}_m^2}}-\pi t^-\frac{\tilde{\Delta}_n}{\sqrt{\tilde{\omega}_n^2+\tilde{\Delta}_n^2}} \tag{6}$$

and

$$\tilde{\omega}_n=\omega_n+\pi T\sum_{m=-\infty}^{\infty}\lambda(n-m)\frac{\tilde{\omega}_m}{\sqrt{\tilde{\omega}_m^2+\tilde{\Delta}_m^2}}+\pi t^-\frac{\tilde{\omega}_n}{\sqrt{\tilde{\omega}_n^2+\tilde{\Delta}_n^2}}\ , \tag{7}$$

with the same notation as before. Here, t^- is the magnetic impurity spin-flip scattering rate related to the scattering time τ_P for paramagnetic impurities by $t^-\equiv1/(2\pi\tau_P)$. The function $\lambda(n-m)$ is related, in the usual manner, to the electron-phonon spectral density $\alpha^2F(\Omega)$ by

$$\lambda(n-m)=\int_0^\infty \frac{2\Omega\alpha^2F(\Omega)}{\Omega^2+(\omega_n-\omega_m)^2}d\Omega \ . \tag{8}$$

Equations (1)–(3) reduce in the static limit to the above equations for paramagnetic impurities by choosing for the form of $P(\omega)$

$$P(\omega)=A_P\omega\delta(\omega) \ . \tag{9}$$

We use this in the definition for $\lambda^{\pm}(n-m)$:

$$\lambda_P^{\pm}(n-m)=\pm 2\int_0^\infty d\omega \frac{\omega P(\omega)}{\omega^2+(\omega_n-\omega_m)^2} \ , \tag{10}$$

which for $n=m$ gives $\lambda_P^{\pm}=\pm A_P$ and for $n\neq m$ yields $\lambda_P^{\pm}=0$. Therefore,

$$\pi T\sum_m \lambda_P^{\pm}(n-m)\frac{\tilde{\omega}_m}{(\tilde{\Delta}_m^2+\tilde{\omega}_m^2)^{1/2}}=\pm\pi T A_P\frac{\tilde{\omega}_n}{(\tilde{\Delta}_n^2+\tilde{\omega}_n^2)^{1/2}} \ , \tag{11}$$

which make Eqs. (1)–(3) equivalent to Eqs. (6)–(8) for $A_P=t^-/T$, at finite T.

Nass *et al.*[9] (see also Schachinger *et al.*[10] and Stephan and Carbotte[11]) have employed the standard form of the Eliashberg equations formulated for paramagnons and have introduced the spin-glass nature of the system through their choice of the spectral density for the spin fluctuations $P(\Omega)$, where a weak exchange interaction occurs between the local moments and the conduction electrons.

Following the example of Dzyaloshinskii and Volovik,[31] they model the electron-spin spectral density by a dynamic contribution equivalent to the hydrodynamic limit of a Heisenberg paramagnet[32–35] and a static component in the form of a Dirac delta function at zero frequency which represents spin freezing.

The electron -spin spectral density $P(\Omega)$ that enters the Eliashberg equations is related to the spin spectral density $B(q,\Omega)$ by

$$P(\Omega)=N(0)J^2\int_0^{2k_F}\frac{q\,dq}{2k_F^2}B(q,\Omega) \ , \tag{12}$$

where J is the electron magnetic impurity exchange constant, which couples the superconducting electron to the magnetic impurity.

The spin spectral density that Nass *et al.*[9] suggest is given as

$$B(q,\omega)=B_d(q,\omega)+B_s(q,\omega) \ , \tag{13}$$

where the dynamic part is given as

$$B_d(q,\omega)=\frac{D\chi\omega q^2}{\omega^2+(Dq^2-\omega^2\tau)^2} \tag{14}$$

and the static part is given by

$$B_s(q,\omega)=\pi(1-e^{-\beta\omega})\tilde{Q}(T)\delta(\omega) \ . \tag{15}$$

Here, D is the spin diffusion constant, χ is the static susceptibility, which is taken to be independent of q, and τ is a phenomenological magnetic relaxation time that is used as a cutoff in the sum rules that apply to this spectral density.[9,11,33,34] In Eq. (15), $\tilde{Q}(T)$ is the temperature-dependent Edwards-Anderson order parameter.[5] Two models for the temperature dependence have been suggested for this quantity. Edwards and Anderson[5] have derived its temperature dependence from a mean-field solution and find

$$\tilde{Q}(\bar{t})=S^2(1-\bar{t}) \ , \tag{16}$$

where $\bar{t}=T/T_f$ and S is the impurity spin. Nass *et al.*[9] have also suggested the form

$$\tilde{Q}(\bar{t})=S^2(1-\bar{t}^2) \ . \tag{17}$$

If the spin-glass parameters χ, D, and τ are allowed to vary arbitrarily, unphysical results are found for the tunneling density of states[9] and in the transport properties.[32] Therefore, two sum rules are imposed on the spin-spectral density $B(q,\omega)$. The one is the standard f-sum rule[35] and the other is a sum rule arising from the definition of the structure factor.[9] Rather than review these results here, we prefer to refer the reader to the literature,[9,11] where detailed discussion of the sum rules exist and their evaluation for several spin-glass parameters has been performed.

Keller,[36] in the case of a ferromagnet, and Nass *et al.*[9] have found, in the case of the above model, that the terms for $\lambda(n-m)$, where $n\neq m$ in the dynamic part of the Eliashberg equations are negligible compared to the $n=m$ term $\lambda(0)$ and hence it is only necessary to keep the $n=m$ term in the Matsubara frequency sums. Thus, $\lambda_d(0)$ can be evaluated using the sum rules[11] to be

$$\lambda_d(0)=N(0)J^2\pi\chi \ . \tag{18}$$

It can be shown, from applying the procedure outlined in Eqs. (9)–(11) to Eqs. (12)–(15), that the problem has now been reduced from one of dynamic spin fluctuations to one of temperature-dependent static impurity scattering where

$$\begin{aligned}\frac{1}{2\pi\tau_P}&=T\lambda(0)\\&=T[\lambda_d(0)+\lambda_s(0)]\\&=N(0)J^2\pi[T\chi+\tilde{Q}(\bar{t})] \ .\end{aligned} \tag{19}$$

Therefore, we are now solving the standard Eliashberg equations modified for Abrikosov-Gor'kov impurities, $\alpha=1/\tau_P$, but now α is temperature-dependent [i.e., $\alpha\rightarrow\alpha(T)$] and is given by

$$\alpha(T)\propto T\lambda(0) \ , \tag{20}$$

and the effective scattering rate t^{sg} in the spin-glass state is reduced from the Abrikosov-Gor'kov scattering rate t^{ag} (using the notation $t^-\equiv t^{ag}$) by

$$t^{sg}=t^{ag}\frac{\alpha(T)}{\alpha(T_c)} \ . \tag{21}$$

Finally, we need a model for the freezing temperature in terms of the concentration of impurities. This is taken from the experimental observation that T_f is proportion-

al to the concentration of impurities:

$$T_f = \frac{n_i}{n_c} R T_c^0 , \tag{22}$$

where n_i is the Abrikosov-Gor'kov impurity concentration and n_c is its critical value which reduces T_c to zero. T_c^0 is the T_c in the absence of impurities and R is a dimensionless constant between 0 and 1.

III. THERMODYNAMIC PROPERTIES

In what follows here, we will be using results previously obtained by Stephan and Carbotte[11,37] for the temperature-dependent scattering rate. Stephan and Carbotte solved for the temperature dependence of $\alpha(T)$ for several values of the spin-glass parameters R, D, τ, and either $\tilde{Q}(\bar{t})=S^2(1-\bar{t})$ or $\tilde{Q}(\bar{t})=S^2(1-\bar{t}^2)$. We have chosen only two of these cases to illustrate the two possible temperature-dependent scenarios that are likely to occur in this model. For a knowledge of how these quantities might vary with a change in one or the other of the spin-glass parameters, the reader should consult the work of Stephan and Carbotte.[11,37] Here, we use the scattering rate t^{sg}_{-} given in Eq. (21) in replacement of t^{-} in Eqs. (6) and (7) to calculate superconducting properties in Eliashberg theory and, in addition, to examine properties not previously investigated by Stephan and Carbotte.[11]

In Fig. 1 we show the temperature dependence of the scattering rate $\alpha(\bar{t})$ normalized to its infinite temperature limit $\alpha(\infty)$, for two sets of parameters, which we will call case 1 (solid line) and case 2 (dashed curve). Here $\bar{t}=T/T_f$. In case 1, the dimensionless spin-glass parameters are $\bar{D}(1)=D(2k_F)^2/T_f=1$, $\tilde{Q}(\bar{t})=S^2(1-\bar{t}^2)$, $R=0.1$, and $\bar{\tau}=T_f\tau=0.2$. In case 2, $\bar{D}(1)=2$, $\tilde{Q}(\bar{t})=S^2(1-\bar{t})$, $R=0.4$, and $\bar{\tau}=0.2$. These curves and others similar to them have already been presented by Stephan and Carbotte.[11,37]

In Fig. 1, the scattering rate reduces from the high-temperature limit with significant reduction occurring below T_f as the spins freeze into a random configuration and are unavailable to spin-flip scatter. In case 2, the rate dips and then recovers producing reentrant phenomena as we will later discuss. The detailed shape of the curve is due to the interplay between the dynamic and static contributions to the scattering rate in the low-temperature region. The zero-temperature limit of the scattering rate is proportional to S^2, whereas the high-temperature limit proportional to $S(S+1)$, hence the ratio of $\alpha(\bar{t})/\alpha(\infty)$ approaches $S^2/[S(S+1)]$ at zero temperature. In this work we have followed Stephan and Carbotte[11,37] and have used $S=\frac{5}{2}$ (keeping Ag-Mn in mind). As a result, these curves approach a value of 0.714 28 at $\bar{t}=0$.

In Fig. 2 we show the T_c curves, for these models as a function of impurity scattering or concentration t_-, which resulted when we solved the Eliashberg equations with the temperature-dependent scattering rate given in Fig. 1. Again, the solid curve corresponds to case 1 and the dashed curve to case 2. The dotted curve is the Abrikosov-Gor'kov curve that results for the same parameters but with no temperature dependence in the impurity scattering [i.e., $\alpha(T)=\alpha(\infty)$ in Eq. (21)]. Here we have used in the Eliashberg equations a delta function for the electron phonon spectral density $\alpha^2F(\omega)=(\omega_E\lambda_E/2)\delta(\omega-\omega_E)$, with $\omega_E=10$ meV, $\mu^*=0$, $T_c^0=11.604$ K $=1$ meV, which sets $\lambda_E=0.9$. One sees the famous Abrikosov-Gor'kov result, that T_c is reduced from its pure value T_c^0 on addition of magnetic impurities. For small concentrations, the dependence of T_c on t_- is linear. There is also a critical concentration at which the superconductivity is destroyed. In the case of the spin glass, the temperature-dependent scattering rate is reduced from the corresponding Abrikosov-Gor'kov rate as the spins freeze, reducing the effectiveness of the impurity spin to break Cooper pairs through spin-flip scattering.

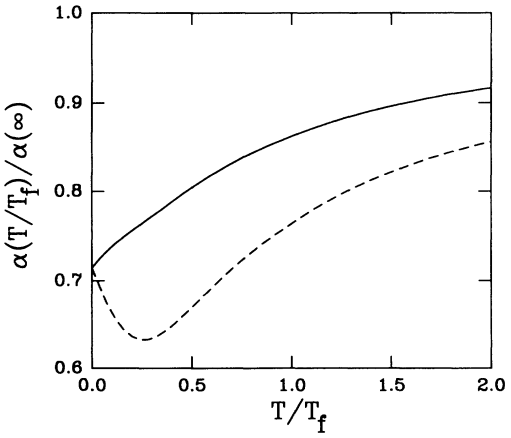

FIG. 1. The temperature dependence of the spin-glass scattering rate $\alpha(\bar{t})$ used in the model in the text normalized to its infinite-temperature limit. Here $\bar{t}=T/T_f$. The solid curve corresponds to what we call case 1 and the dashed curve corresponds to our notation, case 2. In case 1, $\bar{D}(1)=1$, $\tilde{Q}(\bar{t})=S^2(1-\bar{t}^2)$, $R=0.1$, and $\bar{\tau}=0.2$. In case 2, $\bar{D}(1)=2$, $\tilde{Q}(\bar{t})=S^2(1-\bar{t})$, $R=0.4$, and $\bar{\tau}=0.2$.

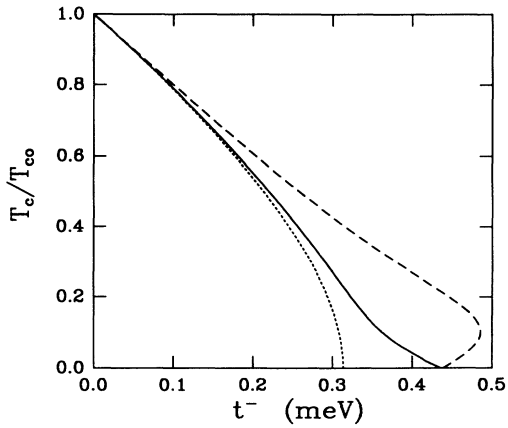

FIG. 2. T_c/T_c^0 vs the magnetic scattering rate t_-. The dotted curve is the Abrikosov-Gor'kov result for the phonon model used in the text. The solid curve corresponds to case 1 in our spin-glass model and the dashed curve corresponds to case 2.

Thus, the spin-glass material may sustain a larger concentration of impurities for the same T_c. The point at which the critical concentration of spin-glass impurities occurs is controlled by the $\bar{t}=0$ point in Fig. 1 or the ratio $S^2/[S(S+1)]$, with the critical $t^{sg}_{\pm}$ equal to $(S+1)/S$ times the critical $t^{ag}_{\pm}$.

Note, that for case 2 (dashed curve) we can expect reentrant phenomena at the lower end of the T_c curve where for the same concentration, two values of T_c exist with a region of superconductivity in between. (Note, that if this diagram were alternatively labeled as a phase diagram with T on the y-axis rather than T_c, then the area to the left of a curve would correspond to the superconducting state and the area to the right the normal state). Reentrant superconductivity is the case where below a temperature T_{c1} a material becomes superconducting but below an even lower temperature $T_{c2}(T_{c2}<T_{c1})$, the material reenters the normal phase again due to the formation of magnetic order, such as ferromagnetism, which inhibits the superconductivity. Examples of reentrant superconductors are $ErRh_4B_4$ (Ref. 38) and $HoMo_6S_8$,[39] where their reentrance is due to a ferromagnetic transition occurring at T_{c2}. In case 2, it is also possible for a spin-glass superconductor to exhibit reentrant phenomena, as has been observed in $La_{1-x}Gd_xRu_2$ by Jones *et al.*[40] Similar theoretical results have been obtained by Soukoulis and Grest.[41]

We will now present results, in these two cases, for the free-energy difference, the thermodynamic critical magnetic field, and the specific heat difference. Similar results have been presented by Stephan and Carbotte[11] for the critical magnetic field, however, our results will go further by extending the parameters into the reentrant region of the model. In all graphs to be presented from here on, we have plotted our results in three-frame figures with the upper frame displaying the Abrikosov-Gor'kov result, the middle frame showing the analogous results for case 1 and the bottom frame for case 2. In addition, the curves in each figure are given for the same set of parameters; we have listed these in Table I. Curves will be presented for six cases: no magnetic impurities $T_c/T_c^0=1.00$ (——), $T_c/T_c^0=0.95$ (----), 0.8 (– – –), 0.58 (— — — —), 0.34 (— – — –), and 0.15 (— – — –). The corresponding Abrikosov-Gor'kov scattering rate $t^{ag}_{\pm}$ and spin-glass scattering rate $t^{sg}_{\pm}$ for each case are given in Table I. The freezing temperature T_f with respect to T_c is also given for the two spin-glass cases.

With our parameters now defined, we will proceed to present results for various thermodynamic quantities: the free-energy difference, the thermodynamic critical magnetic field, and the electronic specific heat difference. These results are based upon a calculation of the free energy. The difference in free energy between the superconducting and normal state ($\Delta F=F_S-F_N$) is given in terms of the Matsubara gaps and frequencies, which follow from the solution of the Eliashberg equations modified for the spin-glass contribution, by the Bardeen-Stephen formula:[42]

$$\Delta F=-N(0)\pi T\sum_{n=-\infty}^{\infty}[(\omega_n^2+\Delta_n^2)^{1/2}-|\omega_n|]\left[Z_S(i\omega_n)-Z_N(i\omega_n)\frac{|\omega_n|}{(\omega_n^2+\Delta_n^2)^{1/2}}\right]. \tag{23}$$

From this the thermodynamic critical magnetic field $H_c(T)$, which is related to the condensation energy of the superconducting state, is given as

$$H_c(T)=(-8\pi\Delta F)^{1/2}. \tag{24}$$

Also, the electronic specific heat difference is given in terms of the free-energy difference by

$$\Delta C(T)=-T\frac{d^2\Delta F}{dT^2}. \tag{25}$$

In Figs. 3 and 4 we plot the difference in free energy ΔF and the thermodynamic critical magnetic field $H_c(T)$, respectively. In both cases we normalized these quantities to the zero-temperature value in the pure case (solid curve). This reduces the plot to dimensionless quantities and permits the reduction in free energy and the corresponding critical magnetic field due to the magnetic impurities to be seen with clarity. The parameters are given in Table I. Frame (a) shows the Abrikosov-Gor'kov results while frames (b) and (c) show the results of case 1 and case 2, respectively, for the spin-glass model used here.

Aside from the overall depression in the magnitude of

TABLE I. Parameters for the curves shown in Figs. 1–9. Case 1 refers to the spin-glass parameters $D=1$, $\tilde{Q}(\bar{t})=S^2(1-\bar{t}^2)$, and $R=0.1$. Case 2 refers to $D=2$, $\tilde{Q}(\bar{t})=S^2(1-\bar{t})$, and $R=0.4$. Parameters used for the pure case are $T_c^0=11.604$ K $=1$ meV, $\omega_E=10$ meV, and $\mu^*=0$.

T_c/T_c^0	$t^{ag}_{\pm}$ (meV)	Case 1 $t^{sg}_{\pm}$ (meV)	Case 1 T_f/T_c	Case 2 $t^{sg}_{\pm}$ (meV)	Case 2 T_f/T_c	Line type
1.00	0.0000	0.0000	0.0000	0.0000	0.0000	————
0.95	0.0246	0.0247	0.0098	0.2478	0.0195	- - - - - -
0.80	0.0945	0.0955	0.0445	0.0976	0.0891	– – – – –
0.58	0.1846	0.1893	0.1200	0.2003	0.2400	— — —
0.34	0.2620	0.2768	0.2905	0.3124	0.5810	– – – – –
0.15	0.3021	0.3409	0.7592	0.4287	1.5183	— - — -

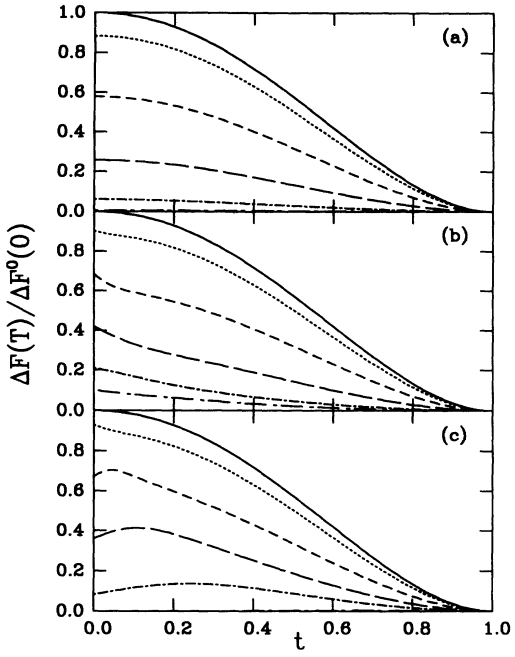

FIG. 3. The free-energy difference ΔF normalized to the zero temperature value in the pure case vs the reduced temperature $t=T/T_c$. (a) Abrikosov-Gor'kov impurities. (b) Spin-glass impurities for case 1. (c) Spin-glass impurities for case 2. See Table I for details of the parameters.

these quantities, we note that at low temperatures in case 1, there is an upturn in the temperature dependence, whereas, in case 2 there is a downturn. The upturn in case 1 reflects the scattering rate steadily decreasing as the temperature is lowered, thus, allowing the superconducting state to lower its energy and become more stable.

On the other hand, in case 2, the scattering rate begins to recover and grow stronger at lower temperatures, thus inhibiting the superconducting pairing. Eventually for large spin-glass impurity scattering we see reentrant behavior [best exhibited in (c) of Fig. 4], where the sample reverts to the normal state at a reduced temperature around 0.35.

On these plots, the features distinguishing case 1 and case 2 are quite strong and, in particular, case 2 has a strong signature with regard to the ordinary Abrikosov-Gor'kov case that should make it observable in experiments.

In Fig. 5 we display results for the calculation of the electronic specific heat difference normalized to the value at T_c. Here the curves exhibit a very strong and unusual temperature dependence. The Abrikosov-Gor'kov curves show a shift upward at higher temperatures with increasing impurity scattering, resulting in the slope of the jump just below T_c decreasing with increased scattering. Overall, the shift in area under the curves reflects the entropy constraint of

$$\Delta S=\int_0^{T_c}\frac{\Delta C}{T}dT=0\ , \tag{26}$$

where ΔS refers to the difference in entropy between the normal and superconducting states which of course must

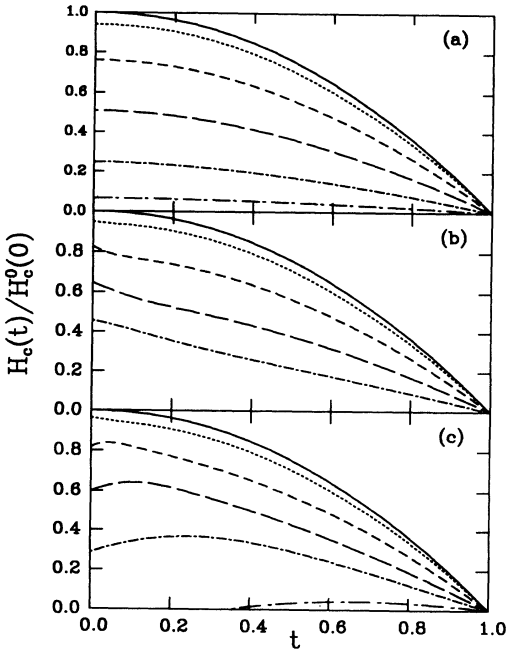

FIG. 4. The thermodynamic critical magnetic field $H_c(T)$ normalized to the zero temperature value in the pure case vs the reduced temperature $t=T/T_c$. (a) Abrikosov-Gor'kov impurities. (b) Spin-glass impurities for case 1. (c) Spin-glass impurities for case 2. See Table I for details of the parameters.

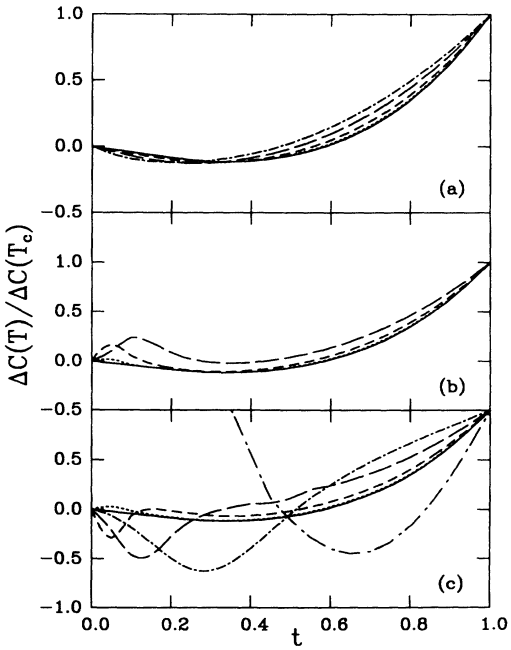

FIG. 5. The electronic specific heat difference $\Delta C(T)$ normalized to its value at T_c vs the reduced temperature $t=T/T_c$. (a) Abrikosov-Gor'kov impurities. (b) Spin-glass impurities for case 1. (c) Spin-glass impurities for case 2. See Table I for details of the parameters.

be zero at T_c [i.e., $\Delta S(T_c)=0$].

For the two cases considered for the spin-glass model there is considerable deviation from the usual temperature dependence with a peak at low temperatures for case 1 and a dip for case 2. Notice again the reentrant behavior in case 2 where the curve returns to a value of 1 (the normal state) at t around 0.35. Also, note that the entropy sum rule above cannot possibly be applied. This is due to the fact that the specific heat presented here is the electronic specific heat, whereas, for the sum rule above, all the contributions to the specific heat must be included, which in this case would include a large magnetic contribution. In practice, this quantity will be difficult to extract experimentally as all other contributions to the specific heat, other than the electronic component, must be subtracted first.

IV. ELECTROMAGNETIC PROPERTIES

In this section we present calculations for several electromagnetic properties, namely, the London and local penetration depths, the electromagnetic coherence length, and finally, the thin-film critical current.

In the case of a superconductor that is sufficiently dirty such that the mean-free path l of the electron is short relative to the zero-temperature coherence length $\xi(0)$ because of impurity scattering, the response of the electrons to an external field is local, and we have the local penetration depth λ_l[43,44]

$$\lambda_l(T)=\left[\frac{8}{3}\pi N(0)e^2v_F^2\tau T\sum_{n=1}^{\infty}\frac{\Delta_n^2}{\omega_n^2+\Delta_n^2}\right]^{-1/2}. \quad (27)$$

Here, v_F is the Fermi velocity, τ is the scattering lifetime, and e is the charge. This can be related to the dc Josephson critical current $J_c(T)$ by[43,44]

$$\frac{J_c(T)}{J_c(0)}=\left[\frac{\lambda_l(0)}{\lambda_l(T)}\right]^2. \quad (28)$$

For nonlocal effects [as in the case of the clean limit where $l\gg\xi(0)$], there are two limits corresponding to either extreme type-I [$\lambda\ll\xi(0)$] or extreme type-II [$\lambda\gg\xi(0)$] superconductivity. The type-I limit is called the Pippard limit and the type-II limit is called the London limit. The formulas for these penetration depths are given in the literature as[43,44]

$$\lambda_P(T)=\frac{4}{3\sqrt{3}}\left[\frac{3\pi^2}{v_F}\frac{n}{m}e^2T\sum_{n=1}^{\infty}\frac{\Delta_n^2}{\omega_n^2+\Delta_n^2}\right]^{-1/3}, \quad (29)$$

for the Pippard penetration depth λ_P, and

$$\lambda_L(T)=\left[\frac{4}{3}\pi N(0)e^2v_F^2T\sum_{n=1}^{\infty}\frac{\Delta_n^2}{Z_n(\omega_n^2+\Delta_n^2)^{3/2}}\right]^{-1/2}, \quad (30)$$

for the London penetration depth λ_L. The temperature-dependent electromagnetic coherence length $\xi(T)$ is given as[43,44]

$$\xi(T)=\frac{v_F}{2}\sum_{n=1}^{\infty}\frac{\Delta_n^2}{Z_n(\omega_n^2+\Delta_n^2)^{3/2}}\Big/\sum_{n=1}^{\infty}\frac{\Delta_n^2}{\omega_n^2+\Delta_n^2}, \quad (31)$$

which can easily be seen to be related to the local and London penetration depths by

$$\xi(T)=l\left[\frac{\lambda_l(T)}{\lambda_L(T)}\right]^2, \quad (32)$$

where $l=v_F\tau$.

In Fig. 6 we show the inverse square of the London penetration depth normalized to the value for the pure case at zero temperature. (Please refer to Table I for the identification of the line types). Note that in case 1 [frame (b)], the magnitude of the curves is increased over the corresponding Abrikosov-Gor'kov case, again reflecting the decreased effective scattering rate. Also in Case 2 [frame (c)] the temperature dependence remains even higher due to a more rapid drop in the scattering rate in this model. Note again the reentrant behavior of the highest concentration case in this figure.

As impurities are added to a system bringing it closer to the dirty limit, the London penetration depth will approach the local limit penetration depth, which already has implicit in it the dirty limit. This is seen upon comparing the dot-long dashed curves in Figs. 6 and 7, which corresponds to the highest impurity concentration used in this model. One cannot see the exact equivalence here as one would in the case of normal impurities, as the concentration of magnetic impurities required would be larger than the critical concentration that destroys the superconductivity entirely.

In Fig. 7 we display the dc Josephson critical current $J_c(T)$ normalized to its pure limit value at zero temperature. This quantity is also the inverse square of the local

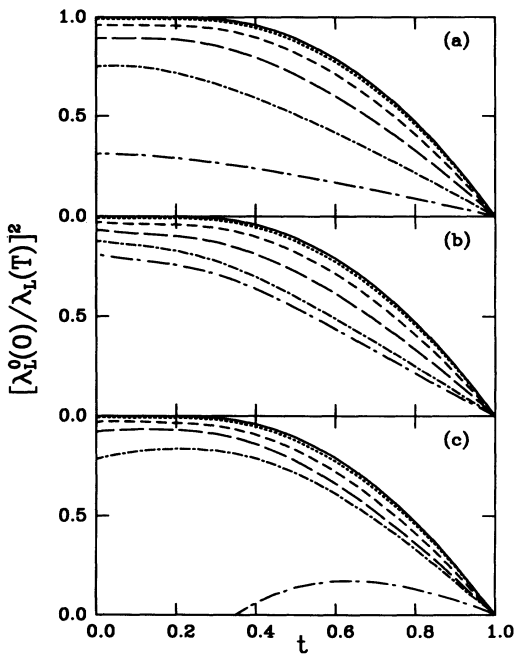

FIG. 6. The inverse square of London penetration depth normalized to the value for the pure case at zero temperature vs the reduced temperature $t=T/T_c$. (a) Abrikosov-Gor'kov impurities. (b) Spin-glass impurities for case 1. (c) Spin-glass impurities for case 2. See Table I for details of the parameters.

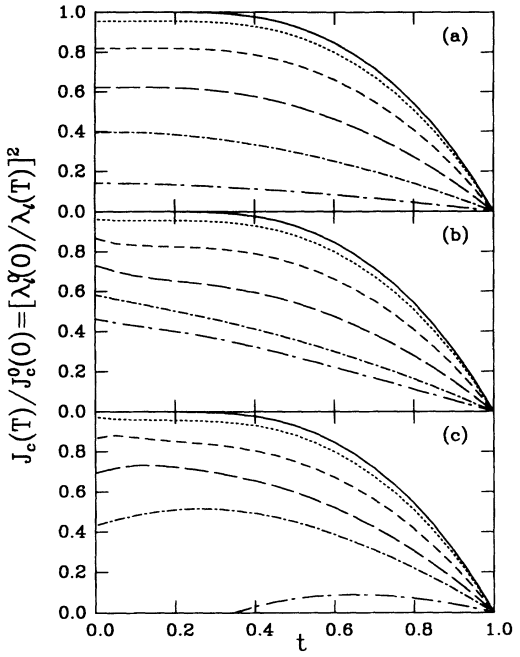

FIG. 7. The dc Josephson critical current $J_c(T)$ normalized to the value for the pure case at zero temperature vs the reduced temperature $t=T/T_c$. (a) Abrikosov-Gor'kov impurities. (b) Spin-glass impurities for case 1. (c) Spin-glass impurities for case 2. See Table I for details of the parameters.

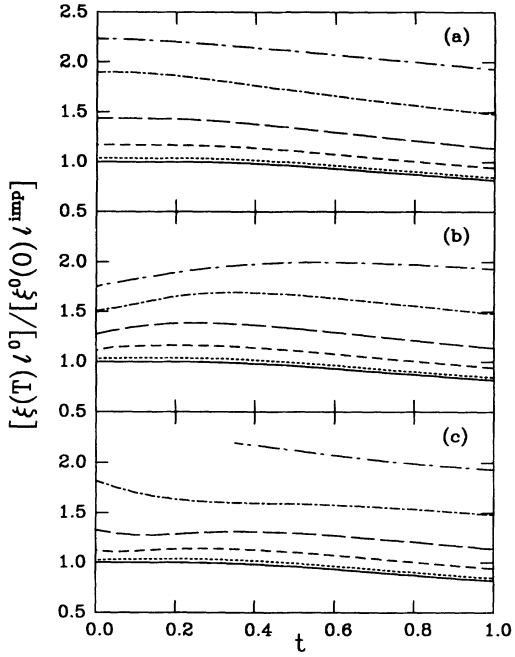

FIG. 8. The temperature-dependent coherence length $\xi(T)$ divided by the mean-free path l^{imp} normalized to the same quantity at zero temperature in the limit of no magnetic impurities, i.e., $\xi(T)l^0/\xi^0(0)l^{imp}$, vs the reduced temperature $t=T/T_c$. (a) Abrikosov-Gor'kov impurities. (b) Spin-glass impurities for case 1. (c) Spin-glass impurities for case 2. See Table I for details of the parameters.

limit penetration depth. Again similar discussion applies as in Fig. 6, with reentrant behavior exhibited by case 2.

We have not shown the Pippard penetration depth because it closely resembles Fig. 7 as from Eqs. (27) and (28), one can see that the formulas are similar with only a slightly different power law. This particular penetration depth is used when referring to type-I superconductors.

Figure 8 exhibits the temperature-dependent electromagnetic coherence length divided by the mean free path l^{imp} normalized to the same quantity at zero temperature in the limit of no magnetic impurities, i.e., $\xi(T)l^0/\xi^0(0)l^{imp}$. In all cases, magnetic impurity scattering increases the magnitude of this quantity with the temperature dependence once again reflecting the variation in the effective scattering rate. As the mean-free path in the presence of magnetic impurity scattering will be smaller than without such scattering, these curves would then indicate that the coherence length itself is reduced by magnetic scattering.

The thin-film critical current due to velocity pair-breaking in zero magnetic field has been calculated in strong coupling theory by Nicol and Carbotte.[45] In the calculation for a spin-glass superconductor, Eqs. (6) and (7) are modified to include the effect of an applied momentum q_s due to the transport current. The resulting change is to replace terms of the form

$$\frac{\tilde{\omega}_m}{\sqrt{\tilde{\omega}_m^2+\tilde{\Delta}_m^2}} \rightarrow \int_{-1}^{1}\frac{dz}{2}\frac{\tilde{\omega}_m - isz}{\sqrt{(\tilde{\omega}_m - isz)^2+\tilde{\Delta}_m^2}} \tag{33}$$

and

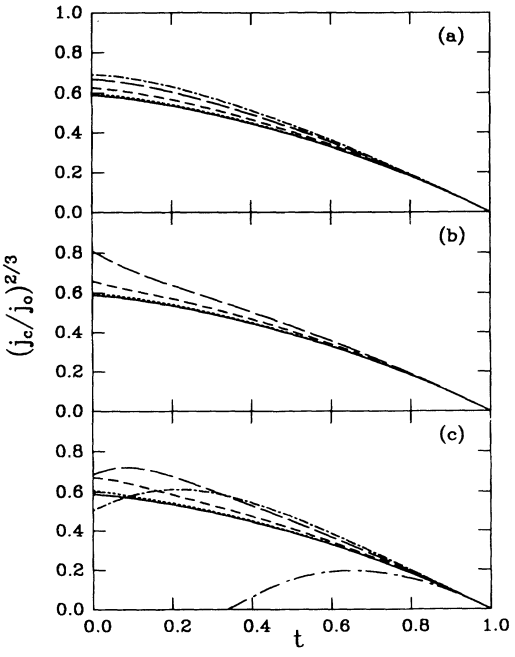

FIG. 9. The thin-film critical current density normalized to the slope at T_c, $(j_0)^{2/3}\equiv -T_c dj_c^{2/3}/dT|T_c$, vs the reduced temperature $t=T/T_c$. (a) Abrikosov-Gor'kov impurities. (b) Spin-glass impurities for case 1. (c) Spin-glass impurities for case 2. See Table I for details of the parameters.

$$\frac{\tilde{\Delta}_m}{(\tilde{\omega}_m^2+\tilde{\Delta}_m^2)^{1/2}} \rightarrow \int_{-1}^{1}\frac{dz}{2}\frac{\tilde{\Delta}_m}{[(\tilde{\omega}_m-isz)^2+\tilde{\Delta}_m^2]^{1/2}}\ , \quad (34)$$

where $s=v_F q_s$ and q_s is the magnitude of the applied momentum of the current. The superfluid current density is then given as[29,45]

$$j_s=\frac{3eN}{2K_F}\pi T\sum_{n=-\infty}^{\infty}\int_{-1}^{1}dz\frac{i(\tilde{\omega}_n-isz)z}{[(\tilde{\omega}_n-isz)^2+\Delta_n^2]^{1/2}}\ . \quad (35)$$

We numerically solve Eqs. (6)–(8), with the above modification, self-consistently for a value of q_s which maximizes j_s. This value of j_s is then defined, in the usual manner, to be the critical current density, j_c.

In Fig. 9 we show the thin-film critical current normalized to its slope at T_c. The formalism for calculating this quantity with the addition of paramagnetic impurities has already been given in Nicol and Carbotte[45] and is described above; we have merely incorporated the temperature-dependent scattering rate into the procedure. It was found previously[45] that the temperature dependence of this quantity is enhanced in the presence of Abrikosov-Gor'kov impurities although the actual magnitude of $j_c^{2/3}$ decreases. One finds that the temperature dependence in the model for case 1 is enhanced over the Abrikosov-Gor'kov result in (a) at low temperatures. For case 2, reentrant behavior occurs as previously discussed.

V. CONCLUSIONS

In conclusion, we have calculated thermodynamic and electromagnetic properties for an intrinsic spin-glass superconductor in the spin-glass model of Nass *et al.*[9] We have extended the BCS calculations of Stephan and Carbotte[11] to strong-coupling Eliashberg theory, so that the theory is capable of providing quantitative predictions. In addition, we have considered properties not previously investigated, to the author's knowledge, within this model.

In general, we find very distinctive behavior in the temperature dependence of the superconducting properties. These should be observable in experiment if this model has any relevance to spin-glass superconductors. In addition, reentrant behavior is a possible signature of a spin-glass state corresponding to case 2 of the model used here.

ACKNOWLEDGMENTS

This work was partly supported by the Natural Sciences and Engineering Research Council of Canada (NSERC) and by the Canadian Institute for Advanced Research (CIAR).

[1]A. A. Abrikosov and L. P. Gor'kov, Zh. Eksp. Teor. Fiz. **39**, 1781 (1960) [Sov. Phys. JETP **12**, 1243 (1961)].
[2]P. W. Anderson and H. Suhl, Phys. Rev. **116**, 898 (1959).
[3]M. B. Maple and O. Fischer, in *Superconductivity in Tenary Compounds II,* edited by M. B. Maple and O. Fischer (Springer-Verlag, Berlin, 1982).
[4]D. Davidov, K. Baberschke, J. A. Mydosh, and G. J. Nieuwenhuys, J. Phys. F **7**, L47 (1977).
[5]S. F. Edwards and P. W. Anderson, J. Phys. F **5**, 965 (1975).
[6]K. Binder and A. P. Young, Rev. Mod. Phys. **58**, 801 (1986).
[7]K. H. Fischer, Phys. Status Solidi B **166**, 357 (1983).
[8]K. Moorjani and J. M. D. Coey, *Magnetic Glassses* (Elsevier, Amsterdam, 1984).
[9]M. J. Nass, K. Levin, and G. S. Grest, Phys. Rev. B **23**, 1111 (1981).
[10]E. Schachinger, W. Stephan, and J. P. Carbotte, Phys. Rev. B **37**, 5003 (1988).
[11]W. Stephan and J. P. Carbotte, J. Low Temp. Phys. **83**, 131 (1991).
[12]A. Perez Gonzalez, E. J. Nicol, and J. P. Carbotte, Phys. Rev. B **45**, 5055 (1992).
[13]N. F. Berk and J. R. Schrieffer, Phys. Rev. Lett. **17**, 433 (1966).
[14]P. B. Allen and B. Mitrović, Solid State Phys. **37**, 1 (1982).
[15]S. Doniach and S. Engelsberg, Phys. Rev. Lett. **17**, 750 (1966).
[16]W. F. Brinkman and S. Engelsberg, Phys. Rev. **169**, 417 (1968).
[17]P. Williams and J. P. Carbotte, Phys. Rev. B **43**, 7960 (1991).
[18]G. Gladstone, M. A. Jensen, and J. R. Schrieffer, in *Superconductivity,* edited by R. D. Parks (Marcel Dekker, New York, 1969), p. 665.
[19]H. Rietschel and H. Winter, Phys. Rev. Lett. **43**, 1256 (1979).
[20]J. M. Daams, B. Mitrović, and J. P. Carbotte, Phys. Rev. Lett. **46**, 65 (1981).
[21]R. Baquero, J. M. Daams, and J. P. Carbotte, J. Low Temp. Phys. **42**, 585 (1981).
[22]B. Mitrović and J. P. Carbotte, Solid State Commun. **41**, 695 (1982).
[23]H. G. Zarate and J. P. Carbotte, Phys. Rev. B **35**, 3256 (1987).
[24]S. Doniach and E.H. Sondheimer, *Green's Functions for Solid State Physicists* (Benjamin, Reading, Mass., 1974).
[25]H. Shiba, Prog. Theor. Phys. 40, 435 (1968).
[26]A. I. Rusinov, Zh. Eksp. Teor. Fiz. **56**, 2043 (1969) [Sov. Phys. JETP **29**, 1101 (1969)].
[27]V. Ambegaokar and A. A. Griffin, Phys. Rev. **137**, A1151 (1965).
[28]S. S. Skalski, O. Betbeder-Matibet, and P. R. Weiss, Phys. Rev. **136**, A1500 (1964).
[29]K. Maki, in *Superconductivity* (Ref.18), p. 1035.
[30]E. Schachinger, J. M. Daams, and J. P. Carbotte, Phys. Rev. B **22**, 3194 (1980).
[31]I. E. Dzyaloshinskii and G. E. Volovik, J. Phys. (Paris) **39**, 693 (1978).
[32]K. H. Fischer, Z. Phys. B **34**, 45 (1979).
[33]H. S. Bennett and P. C. Martin, Phys. Rev. **138**, A608 (1965).
[34]B. I. Halperin and P. C. Hohenberg, Phys. Rev. **188**, 898 (1969).
[35]D. Forster, *Hydrodynamic Fluctuations, Broken Symmetry, and Correlation Functions* (Benjamin, Reading, Massachusetts, 1975).
[36]J. Keller, in *Ternary Superconductors,* edited by G. K. Shenoy, B. D. Dunlap, and F. Y. Fradin (Elsevier–North-Holland,

New York, 1981).
[37]W. Stephan, Ph.D. thesis, McMaster University, 1987 (unpublished).
[38]W. A. Fertig, D. C. Johnston, L. E. DeLong, R. W. McCallum, M. B. Maple, and B. T. Matthias, Phys. Rev. Lett. **38**, 387 (1977).
[39]M. Ishakawa, and O. Fischer, Solid State Commun. **23**, 37 (1977).
[40]T. E. Jones, J. F. Kwak, E. P. Chock, and P. M. Chaikin, Solid State Commun. **27**, 209 (1978).
[41]C. M. Soukoulis and G. S. Grest, Phys. Rev. B **21**, 5119 (1980).
[42]J. Bardeen and M. Stephan, Phys. Rev. **136**, A1485 (1964).
[43]S. B. Nam, Phys. Rev. **156**, 470 (1967).
[44]S. B. Nam, Phys. Rev. **156**, 487 (1967).
[45]E. J. Nicol and J. P. Carbotte, Phys. Rev. B **43**, 10 210 (1991).